AD-A047 571 STANFORD RESEARCH INST MENLO PARK CALIF F/G 14/2

STUDY OF EMP TESTING OF SATELLITES.(U)

SEP 75 S DAIRIKI, W E SCHARFMAN DNA001-74-C-0105

UNCLASSIFIED DNA-4288F NL

1 OF 1

AD

A047571

END

DATE

FILMED

1- 78

DDC

DNA 4288F

(12)

STUDY OF EMP TESTING OF SATELLITES

AD A047571

Stanford Research Institute
333 Ravenswood Avenue
Menlo Park, California 94025

September 1975

Final Report for Period 16 September 1974—15 August 1975

CONTRACT No. DNA 001-74-C-0105

APPROVED FOR PUBLIC RELEASE;
DISTRIBUTION UNLIMITED.

THIS WORK SPONSORED BY THE DEFENSE NUCLEAR AGENCY
UNDER SUBTASK L37DAXYX971-02.

Prepared for
Director
DEFENSE NUCLEAR AGENCY
Washington, D. C. 20305

UNCLASSIFIED

SECURITY CLASSIFICATION OF THIS PAGE (When Data Entered)

REPORT DOCUMENTATION PAGE

READ INSTRUCTIONS BEFORE COMPLETING FORM

1. REPORT NUMBER: 14 12 DNA 4288F
2. GOVT ACCESSION NO.:
3. RECIPIENT'S CATALOG NUMBER:
4. TITLE (and Subtitle): 6 STUDY OF EMP TESTING OF SATELLITES.
5. TYPE OF REPORT & PERIOD COVERED: 9 Final Rep[redacted]t. ~~for Period~~ 16 Sep 74 — 15 Aug 75,
6. PERFORMING ORG. REPORT NUMBER: SRI Project 3077
7. AUTHOR(s): 10 Setsuo/Dairiki, William E./Scharfman
8. CONTRACT OR GRANT NUMBER(s): 15 DNA ~~0~~01-74-C-~~0~~1~~0~~5
9. PERFORMING ORGANIZATION NAME AND ADDRESS: Stanford Research Institute, 333 Ravenswood Avenue, Menlo Park, California 94025
10. PROGRAM ELEMENT, PROJECT, TASK AREA & WORK UNIT NUMBERS: NWET Subtask L37DAXYX971-02
11. CONTROLLING OFFICE NAME AND ADDRESS: Director, Defense Nuclear Agency, Washington, D.C. 20305
12. REPORT DATE: 11 Sep[redacted]75
13. NUMBER OF PAGES: 38 — 12 35p.
14. MONITORING AGENCY NAME & ADDRESS (if different from Controlling Office):
15. SECURITY CLASS. (of this report): UNCLASSIFIED
15a. DECLASSIFICATION/DOWNGRADING SCHEDULE:
16. DISTRIBUTION STATEMENT (of this Report): Approved for public release; distribution unlimited.

16 L37DAXY 17 X971

17. DISTRIBUTION STATEMENT (of the abstract entered in Block 20, if different from Report):

332 500

18. SUPPLEMENTARY NOTES: This work sponsored by the Defense Nuclear Agency under Subtask L37DAXYX971-02.
19. KEY WORDS (Continue on reverse side if necessary and identify by block number): EMP Simulators; Dispersed Pulse; Satellites
20. ABSTRACT (Continue on reverse side if necessary and identify by block number):

Measurements up to 130 MHz in the ARES show non-uniform field variations of 10 dB peak-to-peak. Similar measurements of the field within a 1/30 scale model of the ARES show similar results. Three different scattering structures tested in the ARES model reduce the field non-uniformity caused by signal reflections at equivalent frequencies higher than 30 MHz to less than 3 dB peak-to-peak. Current measurements on models of the structures of the fleet communications satellite in the ARES model indicate that a scattering structure is necessary. Resonances that occur below 25 MHz on the wire top plate of the

DD FORM 1 JAN 73 1473 EDITION OF 1 NOV 65 IS OBSOLETE

UNCLASSIFIED

SECURITY CLASSIFICATION OF THIS PAGE (When Data Entered)

20. ABSTRACT (Continued)

ARES can be tolerated. A potentially inexpensive and effective scattering structure made by stringing wires in the terminating half of the ARES was designed and is recommended for the ARES.

PREFACE

The authors gratefully acknowledge the assistance of Mr. Jon Farber of DNA, who was the Project Officer for this contract. Measurements were performed by Mr. G. Wagner, and the design and construction of the E-field probe by Mr. G. R. Hilbers of Stanford Research Institute.

CONTENTS

ILLUSTRATIONS

TABLE

I INTRODUCTION

This report describes the work performed on a 1/30 scale model of the ARES to obtain information for dispersed EMP testing of satellites in the ARES facility at Kirtland Air Force Base, Albuquerque, New Mexico. The objective of the work was to propagate a dispersed EMP in the ARES that would satisfactorily test satellites. The appendix contains descriptions of H and E field sensors constructed for DNA that will be used for field measurements in the actual ARES.

II PREVIOUS WORK

Final Report 1[1] on work performed through August 1974 describes the non-uniform field existing in the ARES. At frequencies below 25 MHz, the 75 cables that simulate the upper plate of the parallel transmission line resonate strongly since the lines are shorted together at both the input and terminating ends. The resonances may be eliminated by cross-wiring the cables to minimize coupling of signals causing resonance, or by terminating the cables in series resistances that would form matched terminations. In fields produced within the ARES model, cross-wiring [illegible]d by 1-inch by 1-inch mesh (2.5 ft by 2.5 ft full scale) top plate eliminates resonances, but at frequencies above approximately 25 MHz, the field shows non-uniformity in an irregular manner as a function of frequency. The non-uniformity of fields at high frequency may be explained by considering that the signal is propagated as rays, since the vertical dimensions of the ARES are many wavelengths of the signal wavelength. Reflection of the rays from the terminating cone creates constructive and destructive interference locations within the ARES. Efforts to scatter the high-frequency signal with triangular cross-sectional scattering of the structure on the bottom plate of the terminating section and with the mesh top plate were ineffective.

---

[1] S. Dairiki and W. E. Scharfman, "Study of EMP Testing of Satellites," Final Report 1, Contract DNA001-74-C-0105, SRI Project 3077, SRI, Menlo Park, California 94025 (July 1975).

III RECENT WORK ON SCATTERING STRUCTURE WITH MESH TOP PLATE

Since the triangular cross-section scattering structures on the terminating section were ineffective, a round conical shaped scattering structure made of aluminum sheet was constructed, with the base extending halfway into the test section of the ARES model, as illustrated in Figure 1a. Field measurements of the ARES model with the 1-inch by 1-inch mesh top plate showed no improvement in the field non-uniformities at high frequencies. Evidently, a mesh or solid top plate traps most of the high-frequency reflected signals within the ARES, even with the use of a scatterer.

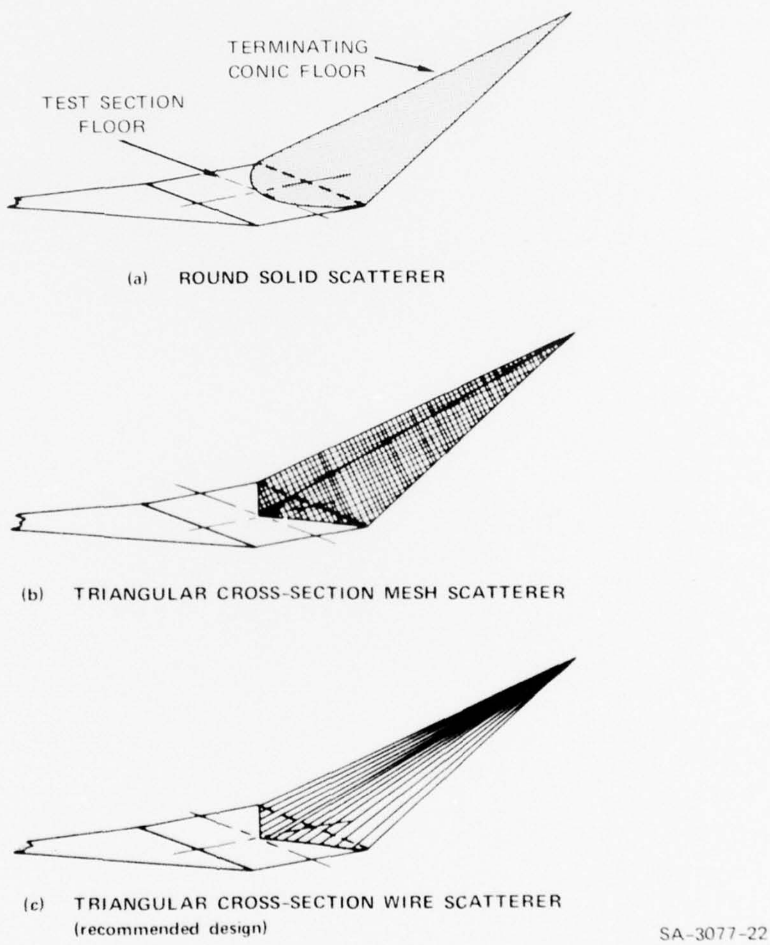

FIGURE 1 SCATTERING STRUCTURES

IV MEASUREMENTS IN THE ARES MODEL WITH WIRE TOP PLATE

A. Field Measurements

High-frequency field measurements were made within the model of the original configuration of the ARES with the 75-wire top plate at several distances from the input terminals of the model and at several heights to obtain vertical profiles of the field variations. Field measurements, compensated for sensor and cable response, are shown in Figure 2, for three-quarters and one-quarter of the height between the bottom and top plates, and at a distance equivalent to 67 meters from the input terminals of the ARES. This location is in the input conic section where the satellite will be positioned. Rapid and largest variations of ±6 dB in field amplitude as a function of frequency occur at one-quarter of the height between the plates rather than near the wires of the top plate where the large variations are caused by resonances for lower frequencies. Similar measurements[2] made on the actual ARES at a slightly different height show 10 dB peak-to-peak variations and are consistent with model measurements.

B. Field Measurements with Scattering Structures

1. Round Conic Scattering Structure

The round conic scattering structure shown in Figure 1a that was ineffective with the mesh top plate is effective with a wire top plate, as illustrated in Figure 3. The variations above 30 MHz have been smoothed and the worst result, which occurs for the one-quarter height,

---

[2] R. Hutchins, BDM, private communication.

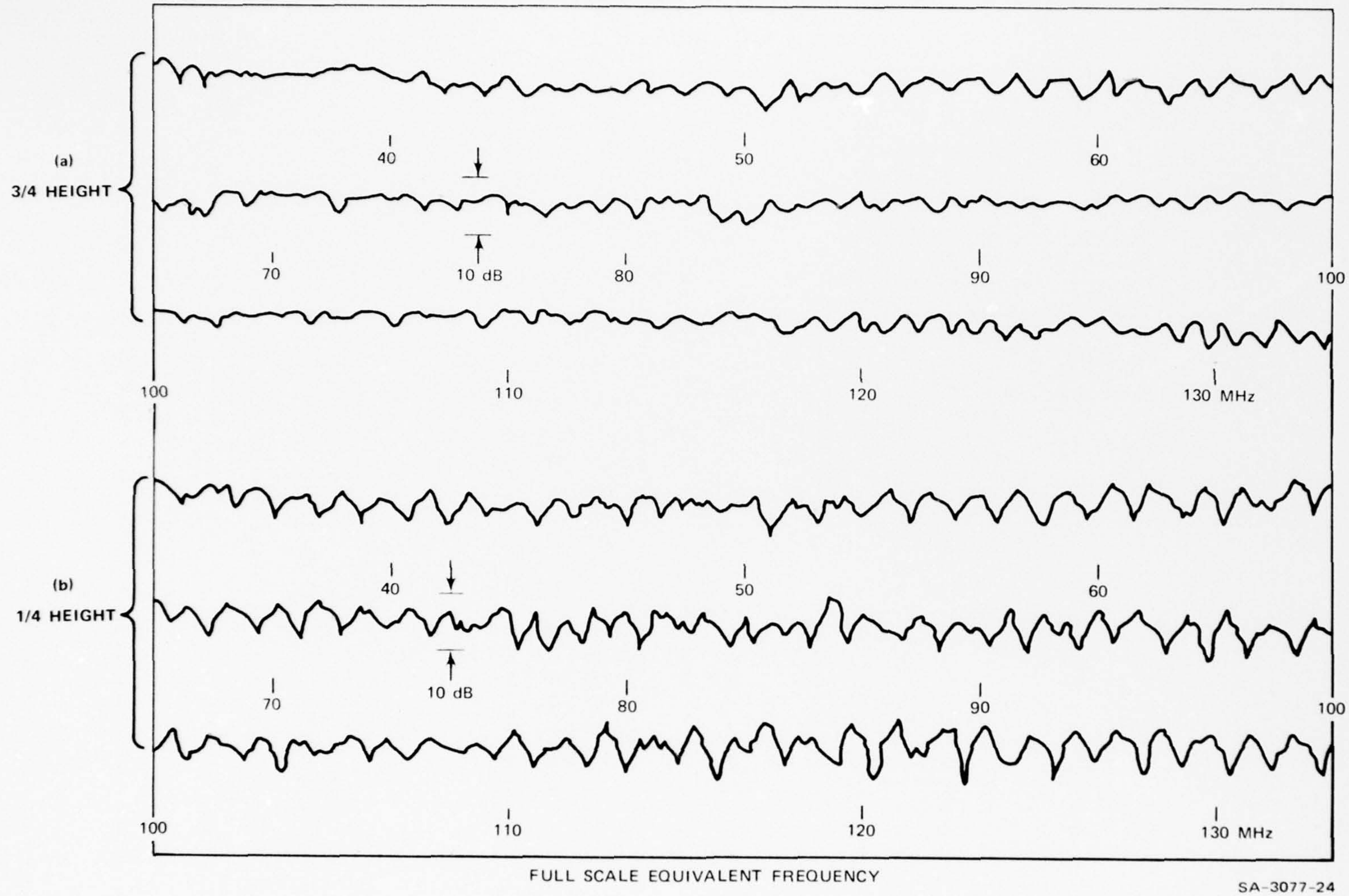

FIGURE 2 FIELD MEASUREMENTS IN ARES MODEL

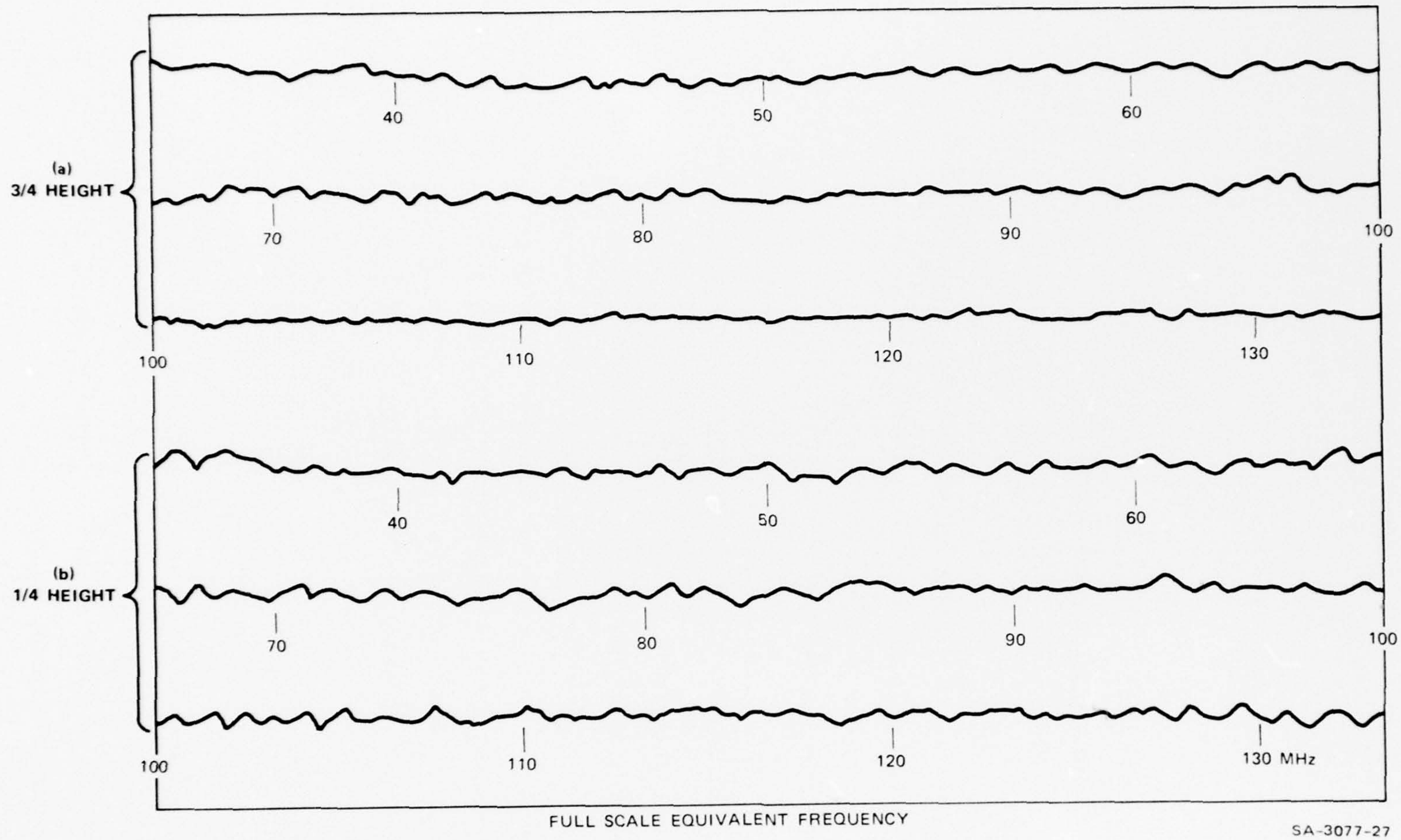

FIGURE 3 FIELD MEASUREMENTS IN ARES MODEL WITH ROUND CONIC SCATTERING STRUCTURE

shows a total variation of ±3 dB over the entire measured frequency range, but shows less than half the total variation over any limited frequency range.

2. Triangular Mesh Conic Scattering Structure

Because of the effectiveness of the curved conic section, a simpler triangular conic section made from one-quarter inch hardware cloth, illustrated in Figure 1b, was investigated as a scattering structure. The vertex of the triangular cone extended to the center of the test floor area. Results of the measurement of the field at one-quarter height, presented in Figure 4, are similar to those for the curved conic section. Grounding or ungrounding the edges of the conic section to the test floor area did not make any perceptible difference.

3. Triangular Wire Conic Scattering Structure

A potentially inexpensive scattering surface for the ARES was simulated by a triangular conic section with 115 wires, as illustrated in Figure 1c. Measurements at one-quarter and three-quarter heights, presented in Figure 5, show that the results are similar to those for the curved and triangular shaped conic sections. For purposes of testing satellites, the modification to the ARES model should include this scattering surface constructed with wires.

C. Current Measurements on Satellite-Like Structures

1. Cylindrical Rod

A cylindrical brass rod, equivalent to a full-scale diameter of 13.7 m by 0.05 m, which is the length of the fleet communications satellite, was centered and placed vertically in the 75-wire top plate ARES model at a distance equivalent to 67 m from the input terminal. A

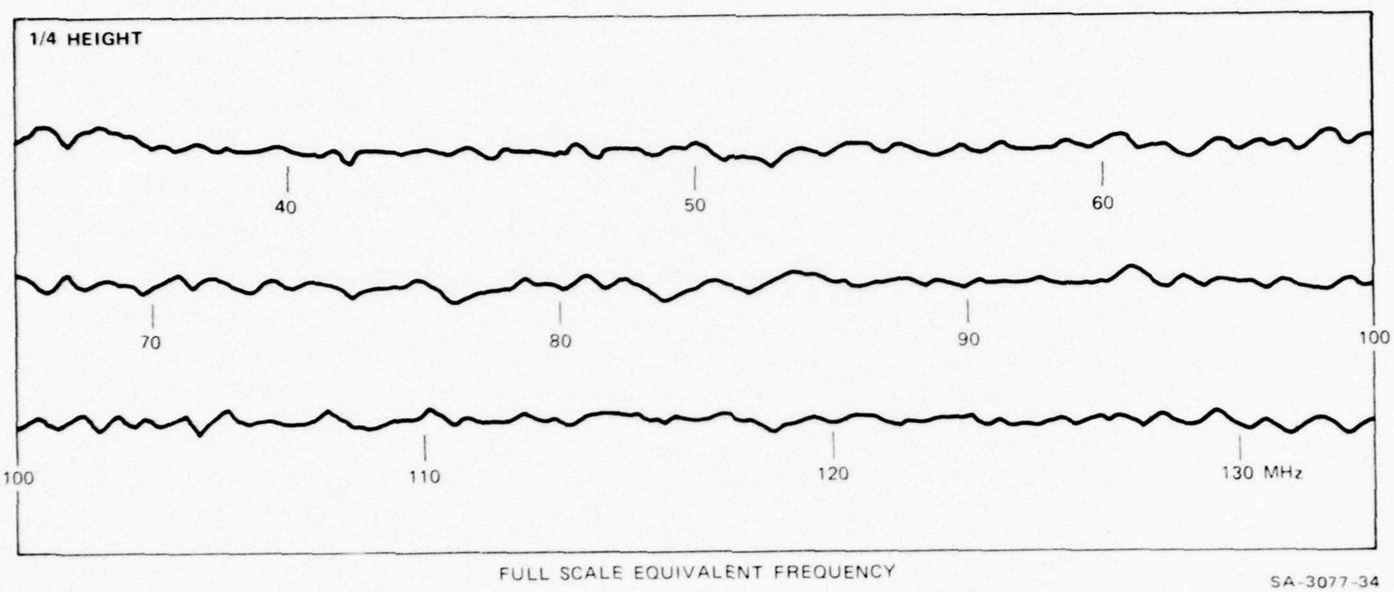

FIGURE 4 FIELD MEASUREMENTS IN ARES MODEL WITH TRIANGULAR MESH CONIC SCATTERING STRUCTURE

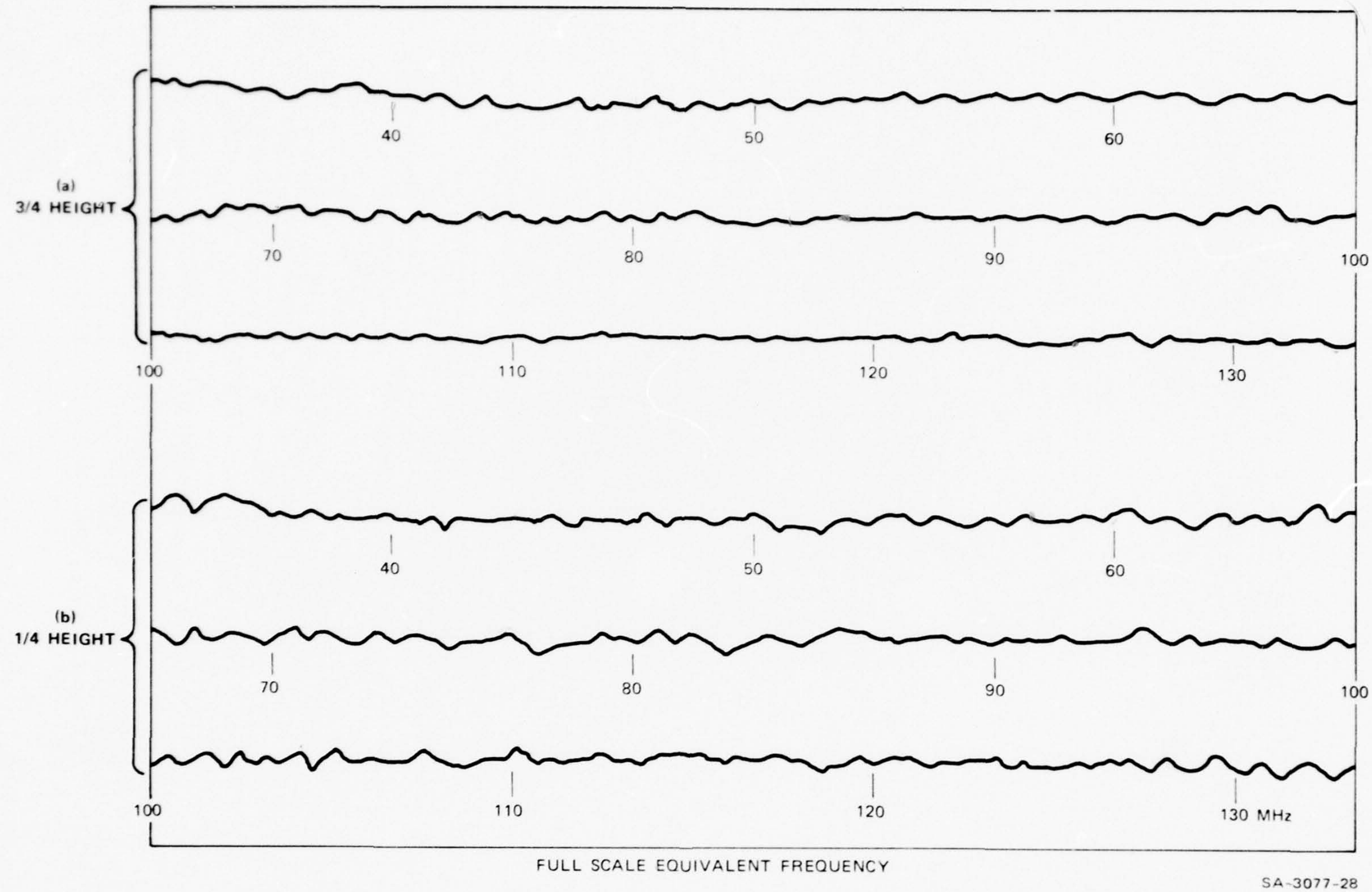

FIGURE 5 FIELD MEASUREMENTS IN ARES MODEL WITH TRIANGULAR WIRE CONIC SCATTERING STRUCTURE

current probe was placed in the middle of the rod. The current amplitudes measured as a function of frequency in the ARES model, with and without the scattering structure, are presented in Figure 6. The current amplitudes are not corrected for probe and cable variations as a function of frequency, and hence they decrease rapidly above the equivalent frequency of 30 MHz. Below an equivalent frequency of about 30 MHz, the current amplitudes as a function of frequency are nearly identical. The peak-to-peak current variation is less than 2 dB down to the satellite EMP lowest significant frequency of 13 MHz. Evidently above 30 MHz, interference effects from ray path reflections cause peaks and nulls in the current induced in the rod when the ARES does not have the scattering structure. The smooth current variation results indicate that reflections are effectively scattered out of the ARES model with the wire top plate by the scattering structure. Measurements with a simulated wooden platform on which the satellite was placed, and measurements with the rod lowered by a quarter of the height between the upper and lower plates of the ARES gave practically identical current variations, indicating that the wooden platform and small vertical displacements are insignificant factors in the measurements.

2. Cylindrical Rod with Simulated Solar Panels

Solar panels, simulated by brass sheets equivalent in dimensions to the solar panels of the fleet communications satellite, were attached to both ends of the 13.7-m by 0.05-m diameter rod. Currents were measured at the center of the vertically positioned rod first with the faces of the panels toward the input terminal and transverse to the length of the ARES and then with the edges of the panels facing the input terminals and longitudinal to the ARES. Figures 7 and 8 show the current amplitudes with and without the scattering structure in the ARES as a function of frequency. The panels electrically load the rod

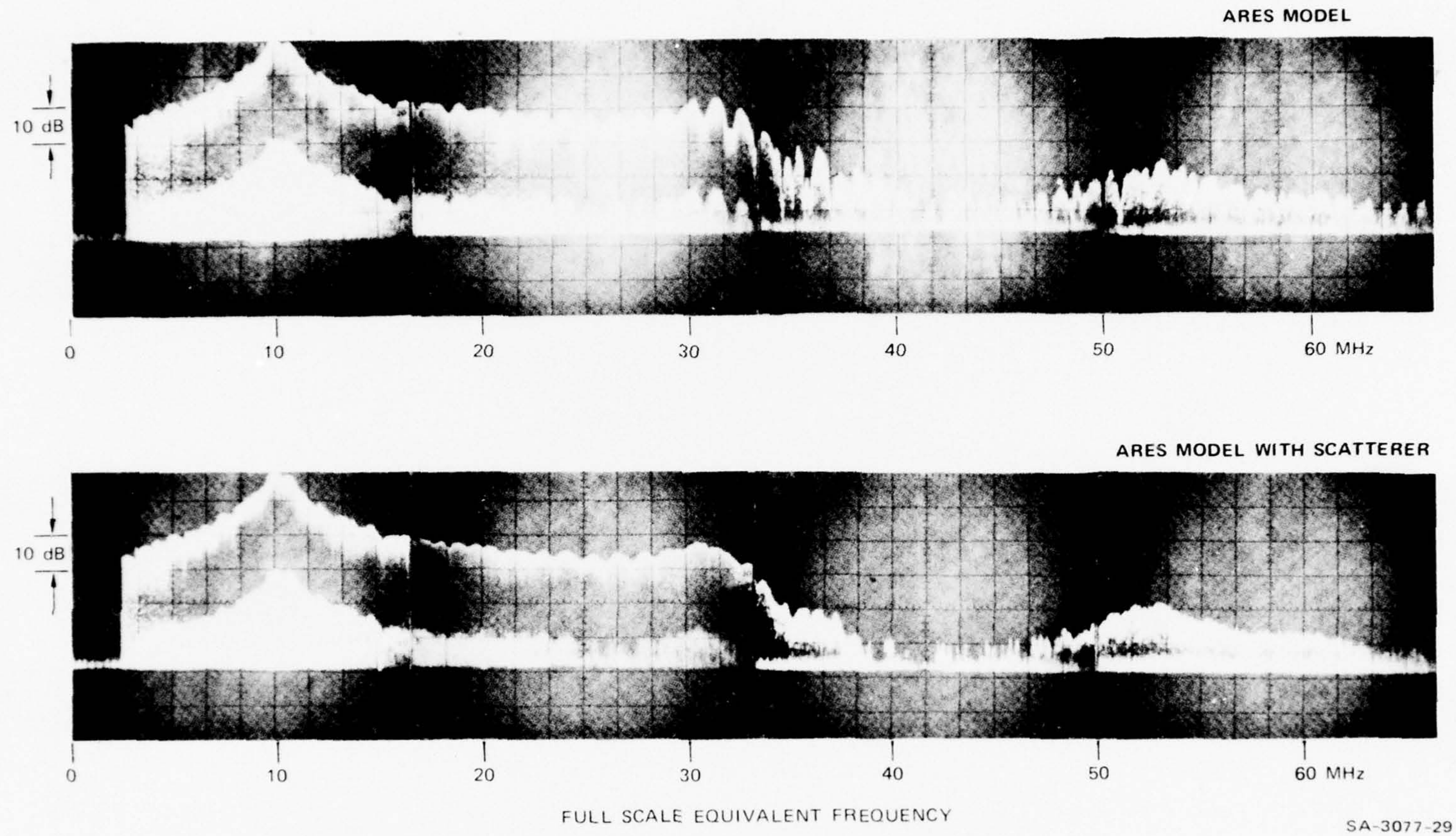

FIGURE 6 CURRENTS ON CYLINDRICAL ROD

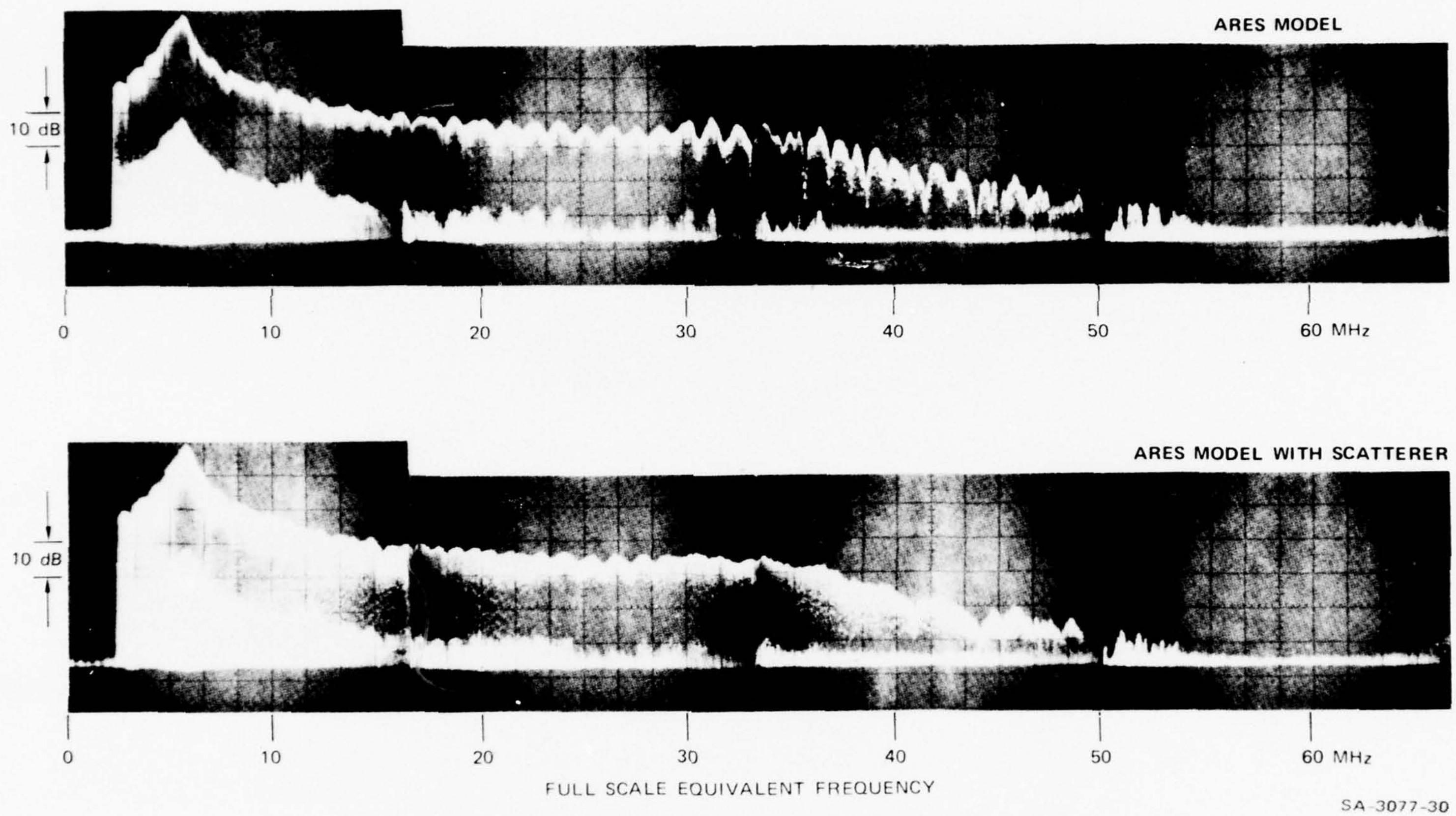

FIGURE 7 CURRENTS ON CYLINDRICAL ROD WITH SOLAR PANELS TRANSVERSE TO LENGTH OF ARES

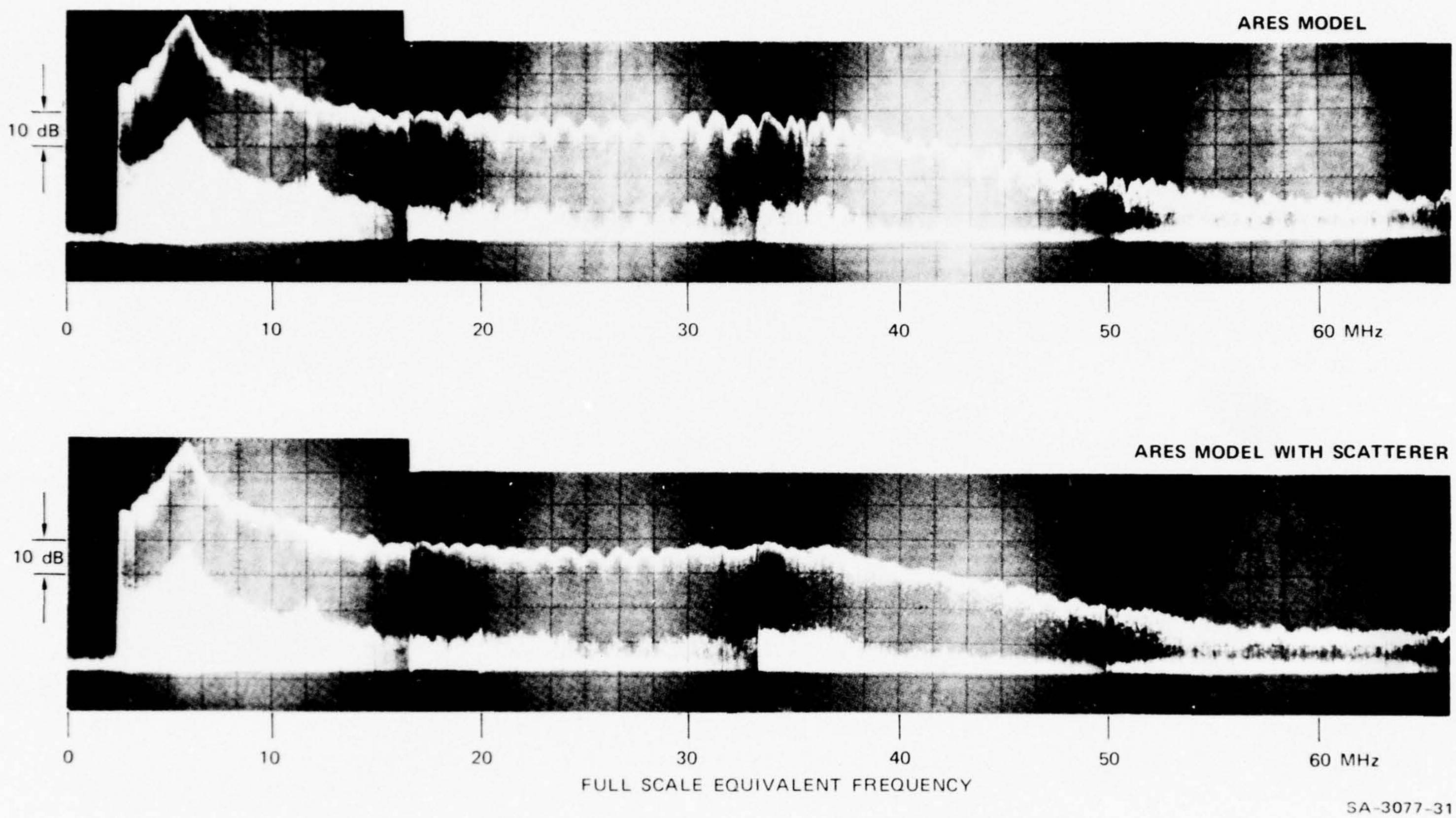

FIGURE 8 CURRENTS ON CYLINDRICAL ROD WITH SOLAR PANELS LONGITUDINAL TO ARES

and cause the fundamental resonance of the rod to shift from 10 MHz to 7 MHz. Current variations in the figures show that the scattering surfaces are necessary for frequencies above 30 MHz. Below 30 MHz the current variations are within ±1.5 dB, and are tolerable.

3. Cylindrical Rod with Panels and Spacecraft Module

A brass box in the shape of a spacecraft module, with a parabolic reflector to model the fleet communications satellite, was added to the rod with solar panels. Instead of being attached to the spacecraft module, the rod passed through it so as to keep the current probe at the same place on the rod. Figure 9 and 10 show the measurements made with the panels both transverse and longitudinal to the ARES and with and without the scattering surface. The effect of the module was to reduce the current variations as a function of frequency in the 30-MHz to 50-MHz range. However, the reduction is insufficient and the scattering structure would be required.

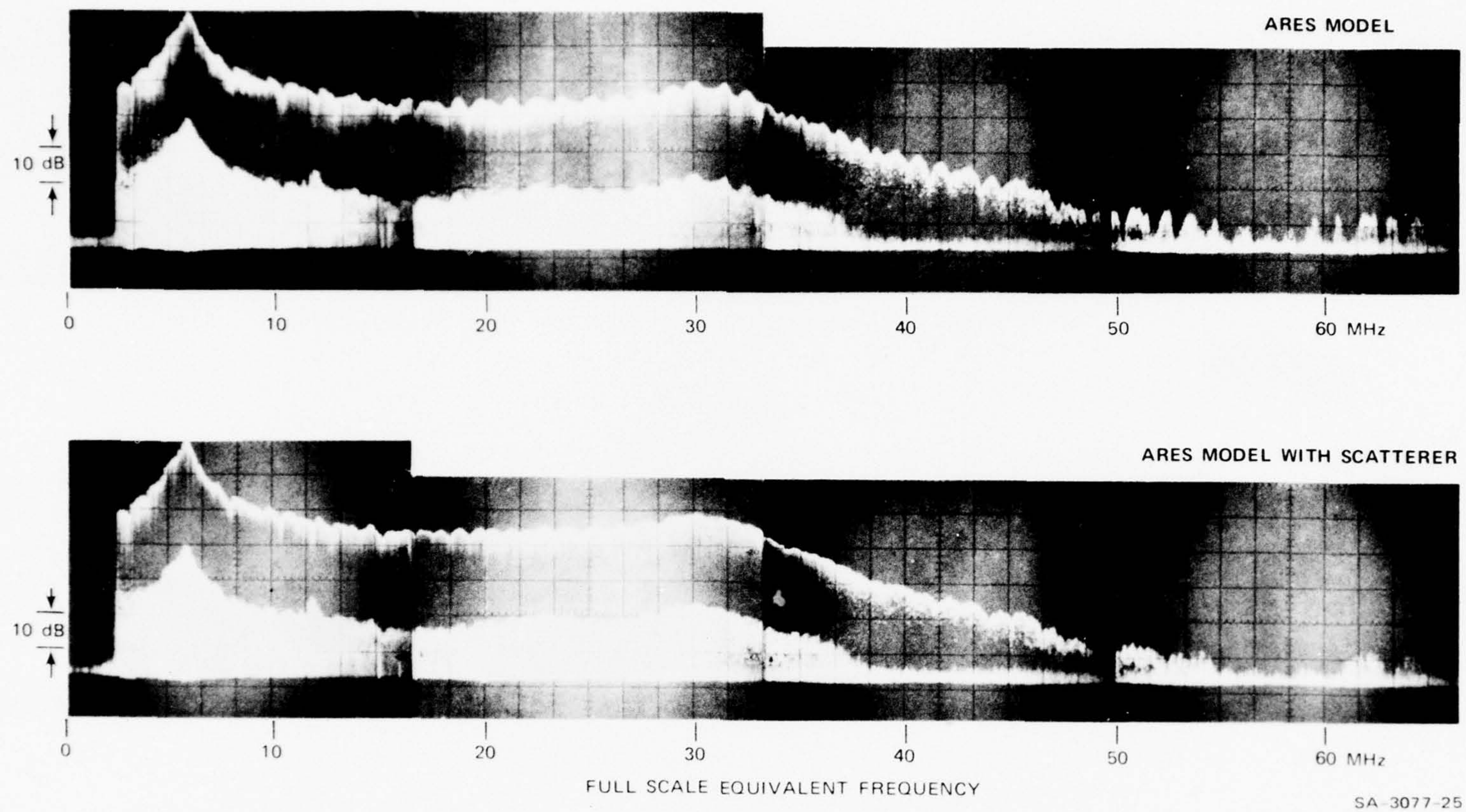

FIGURE 9 CURRENTS ON CYLINDRICAL ROD WITH SPACECRAFT MODULE AND SOLAR PANELS TRANSVERSE TO LENGTH OF ARES

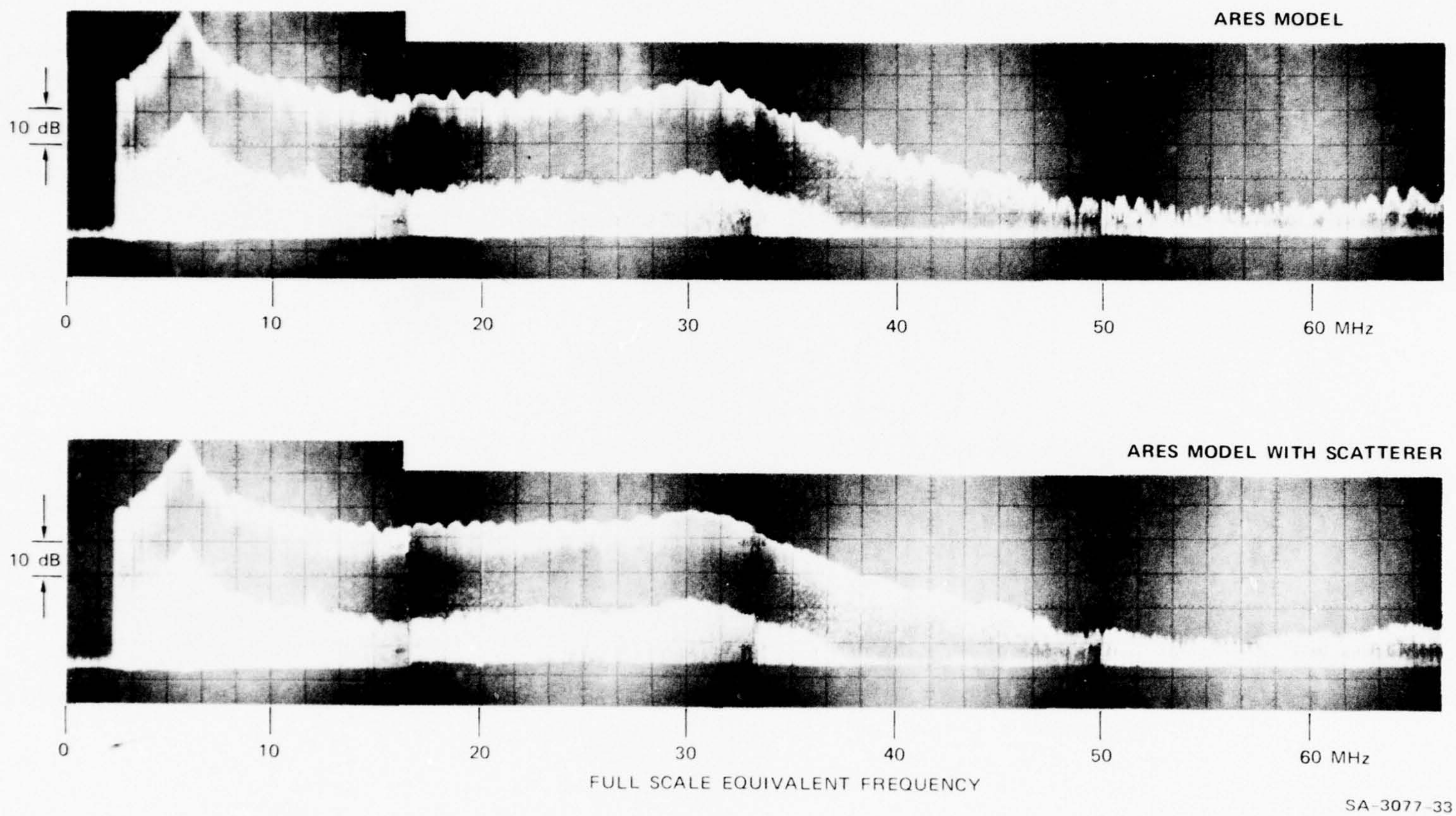

FIGURE 10 CURRENTS ON CYLINDRICAL ROD WITH SPACECRAFT MODULE AND SOLAR PANELS LONGITUDINAL TO ARES

V CONCLUSION

Measurements of the electric fields in the ARES model and of currents on satellite-like models indicate that a scattering structure to reduce the field variation within the ARES is necessary to decrease induced current variations on satellite-like objects for dispersed EMP tests. The 75-cable top plate of the ARES should remain as it is. Cross-wiring the cables eliminates low-frequency resonances but causes the scattering structure to become ineffective. Currents induced on a crude model of a communication satellite indicate that the low-frequency content of the dispersed EMP that causes wire resonances in the ARES are tolerable. These wire resonances could be reduced, if desired, by the addition of series damping resistors, as described in Final Report 1.

Appendix

DESCRIPTIONS OF H AND E FIELD CENSORS

H-Field Probe

The H-field probe (Figure A-1) consists of a metal box with a butterfly slot cut into one side. The slot is shorted in the middle with a wire and the current in the wire is measured with Tektronix CT-1 current probe. The slot is covered with a plastic plate to keep foreign objects out of the box. The output of the box is a GR874 50-ohm connector.

The measured H-field is to be oriented along the slot and perpendicular to the wire. Since the wire short-circuits the slot, the output voltage is proportional to the magnetic field. The ratio of inductance to resistance is high enough that the measured H-field range is nearly independent of frequency from 0.1 MHz to 500 MHz, with the CT-1 current probe causing the frequency dependence below 0.1 MHz.

E-Field Probe

The E-field probe (Figure A-2) consists of a disc-cone shaped probe enclosed in plastic and mounted on the top and bottom of the metal box. The measured E-field is colinear with the disc-cones. The capacitance formed between the disc-cones and the metal box becomes charged by the electric field. Since the output of the disc-cones is applied to the input of a field emission transistor (FET), which has an input impedance much higher than the impedance of the disc-cones, the disc-cones may be considered to be looking into an open circuit. Thus, the outputs of the disc-cones are voltages proportional to the electric field and independent of the frequency.

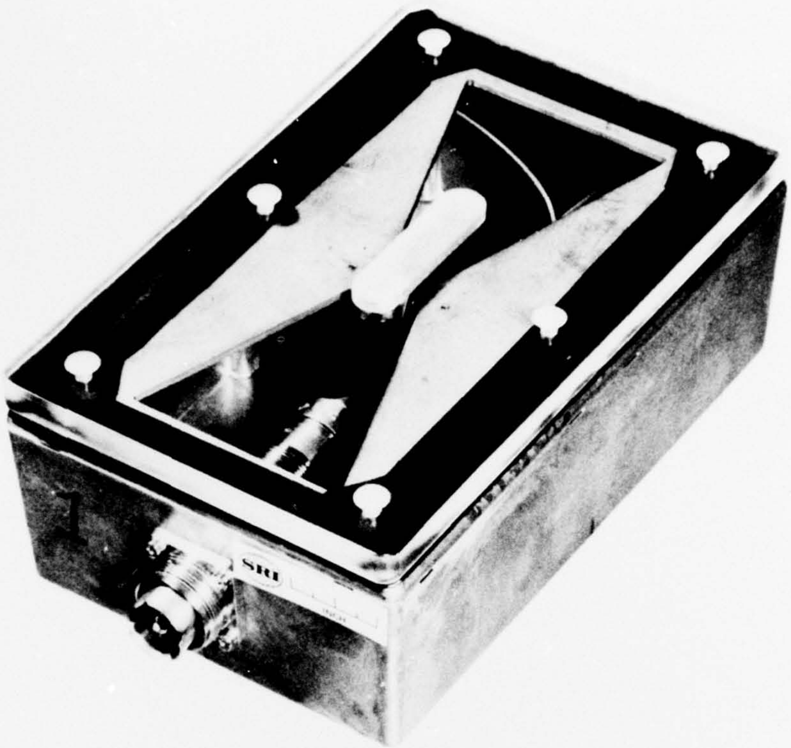

SA-3077-35

FIGURE A-1 H-FIELD PROBE

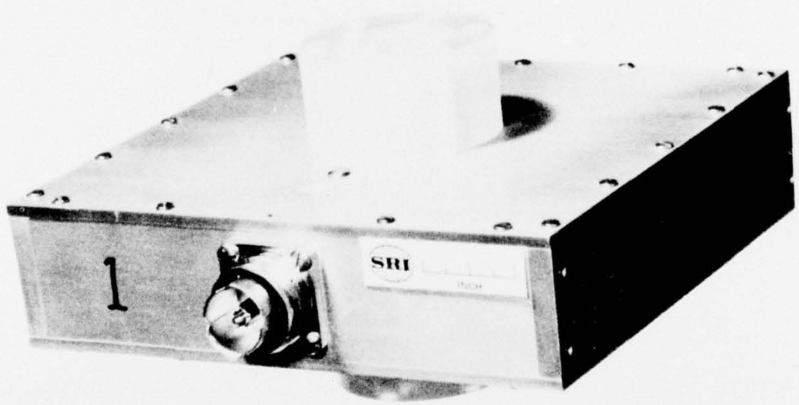

SA-3077-36

FIGURE A-2 E-FIELD PROBE

The schematic diagram of the E-field probe is shown in Figure A-3. The metal box of the E-field probe has a VG1094/U BNC fitting and a GR874 50-ohm connector. The GR874 connector is the output of the probe. The BNC fitting is used as a switch and a charging plug. A BNC shorting plug switches on the battery to supply power for operation. The battery is charged by attaching a cord with a BNC fitting from the charger, as illustrated in Figure A-4.

The instructions for charging are as follows:

- Plug in the SRI-supplied battery charger with switch in charge position.
- Connect charger to probe using cable with BNC type fittings at each end. The meter, which now indicates current in mA, should indicate about 45 mA. An overnight (8-16 hr) charge should be enough for running the probe all day (8-16 hrs).
- Turn switch on charger to battery check position. The meter now indicates voltage with one-half scale equal to about 13 volts.

The instructions for using the E-field probe are as follows:

- Install short circuit BNC plug to charging connector to turn the circuit on.
- Connect RF output cable to probe and measuring instruments.
  - The measured electric field is perpendicular to the broad side of the probe.
  - The output cable should be perpendicular to both the electric field and the direction of the field propagation to minimize cable coupling to the field.

H- and E-Field Probe Calibrations

The H- and E-field probe calibrations were performed in a calibration line that is a small parallel plate transmission line over a ground plane, as illustrated in Figure A-5. The 25-cm height of the parallel plate is less than half the wavelength of the highest design frequency of 500 MHz and aids in reducing the excitation of higher order

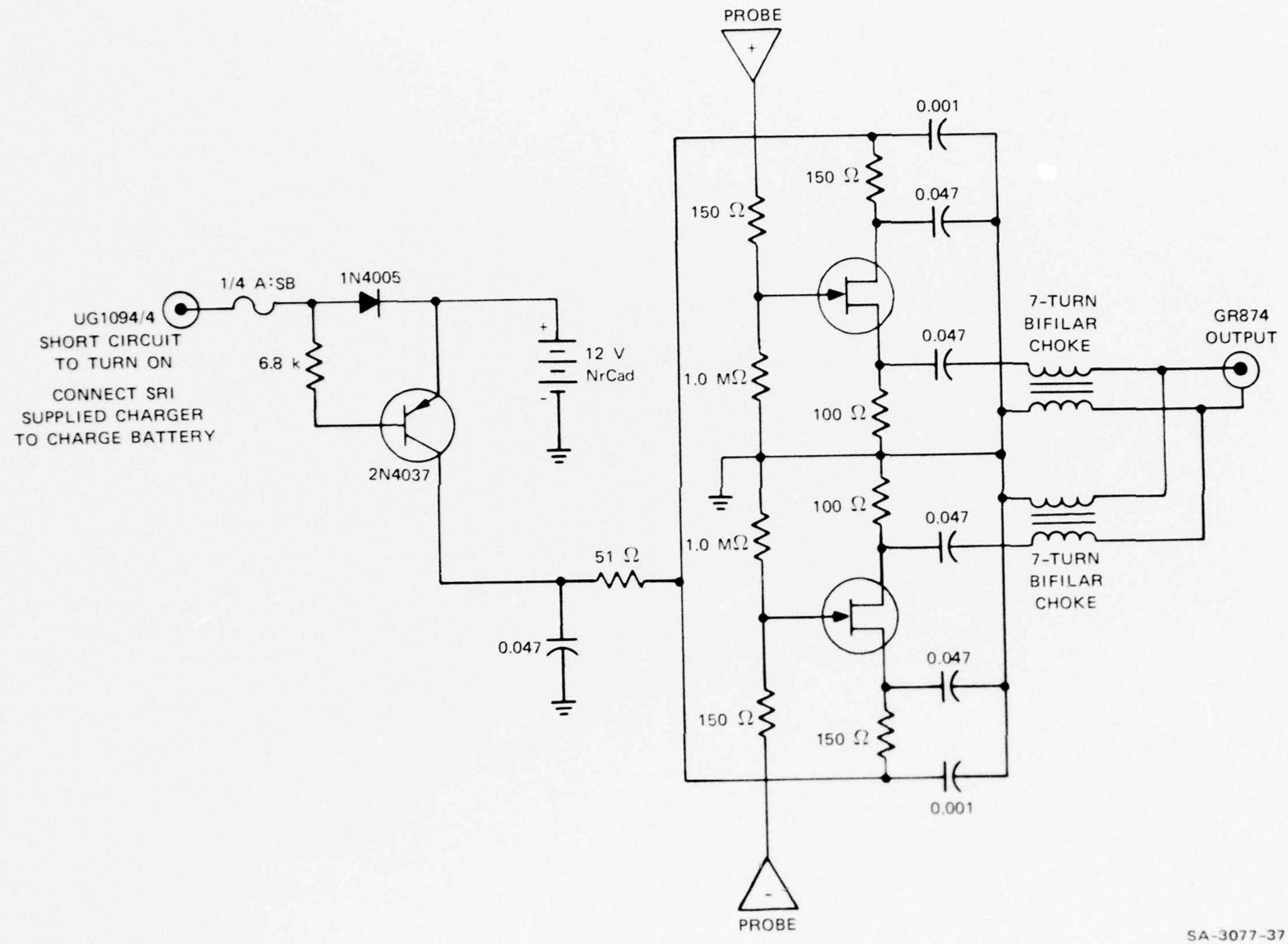

FIGURE A-3 SCHEMATIC OF E-FIELD PROBE

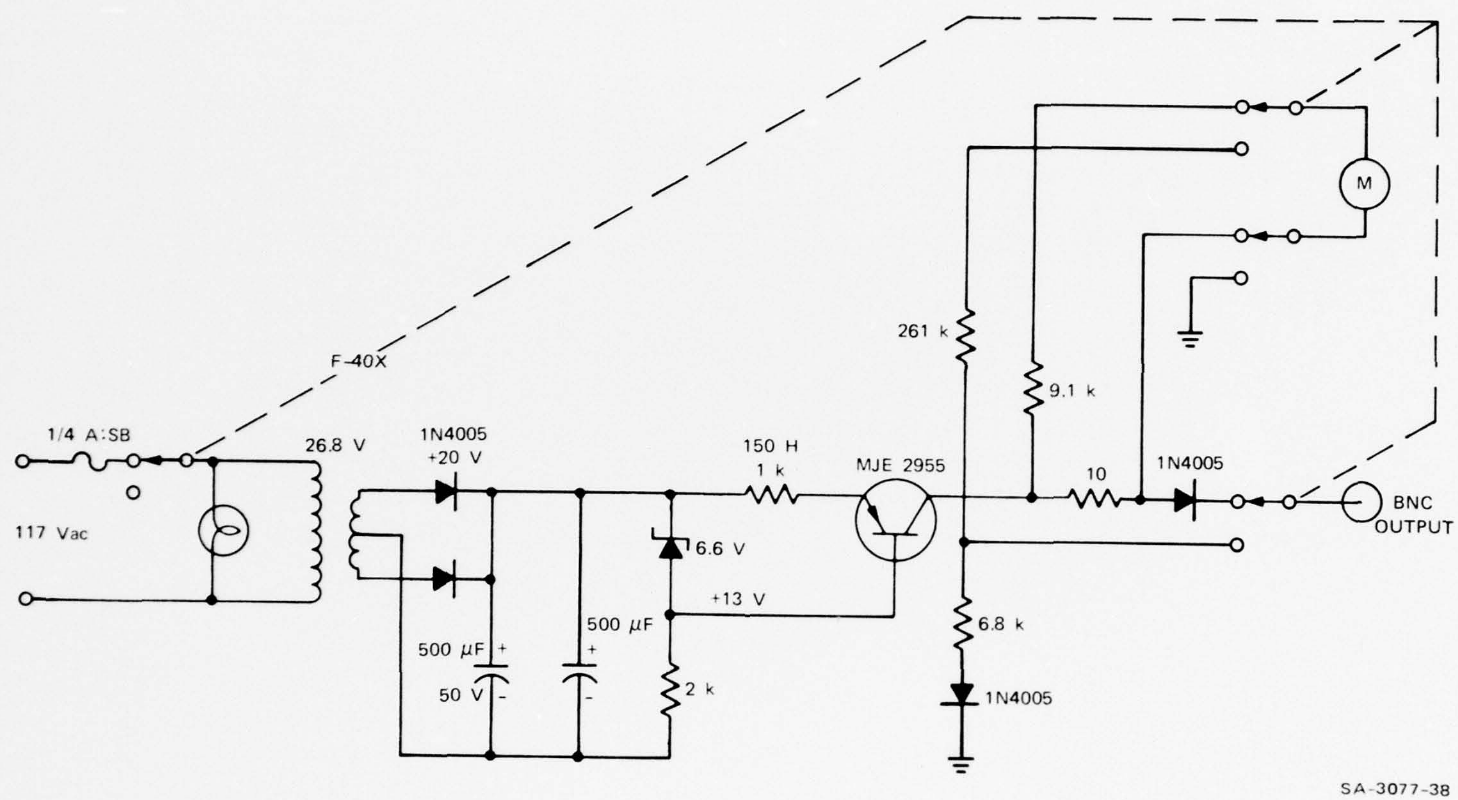

FIGURE A-4 SCHEMATIC OF BATTERY CHARGER FOR E-FIELD PROBE

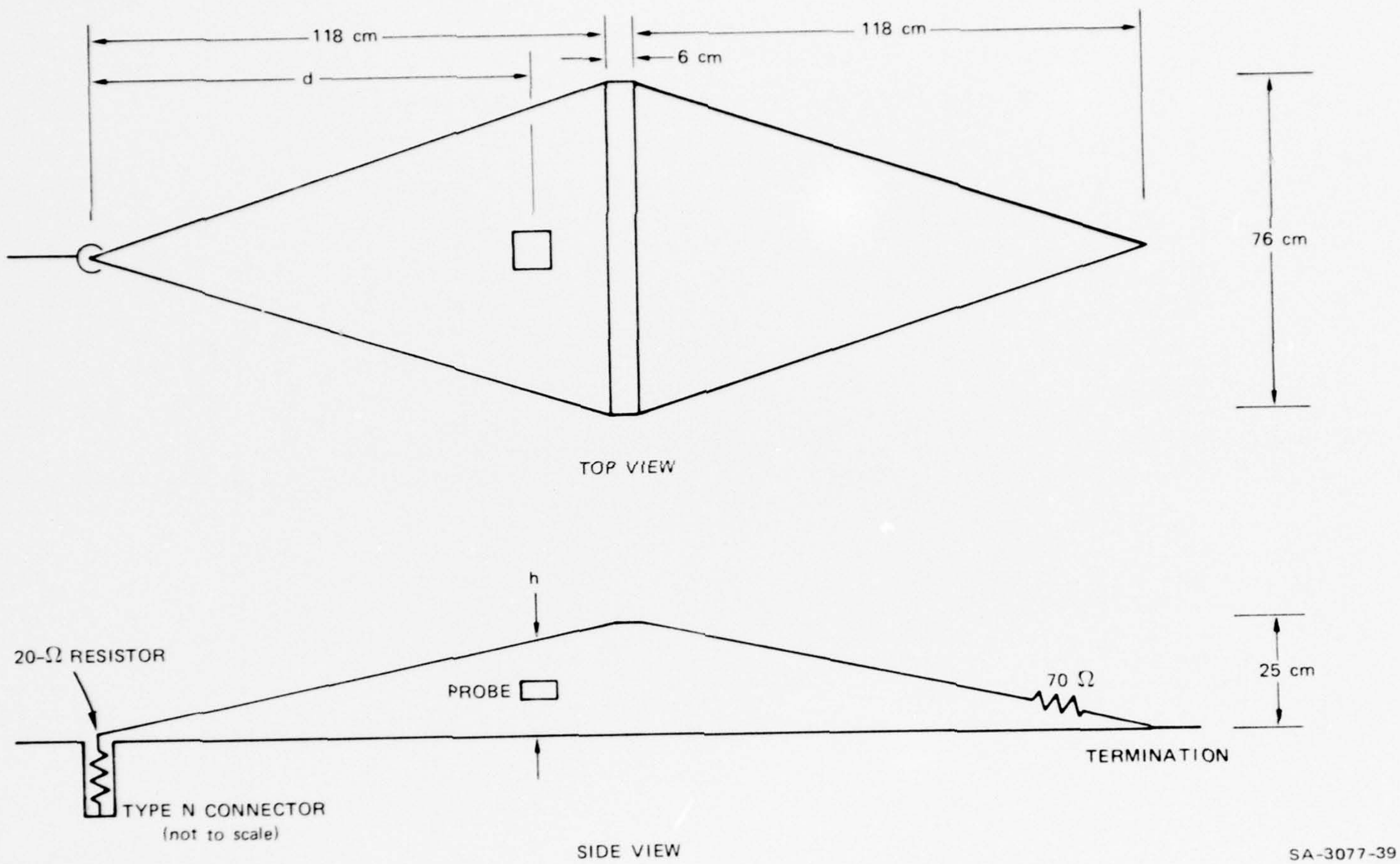

FIGURE A-5 CALIBRATION LINE

modes. Tapered sections 118 cm long connect the parallel plate section, which is 76 cm wide but only 6 cm long, to an input Type N coaxial cable and the termination resistance. Reflectometer measurements gave the best termination resistance for the line of R_L = 70 ohms. The 6-cm length of the parallel section gave the calibration line device best uniform field over the frequency range of 10 MHz to 500 MHz. To absorb reflections at the input end of the tapered section, a resistor, R_S = 20 ohms, was inserted in series with the type N connector at the input end of the tapered section so that a 70-ohm resistance was seen from the input tapered section toward the oscillator.

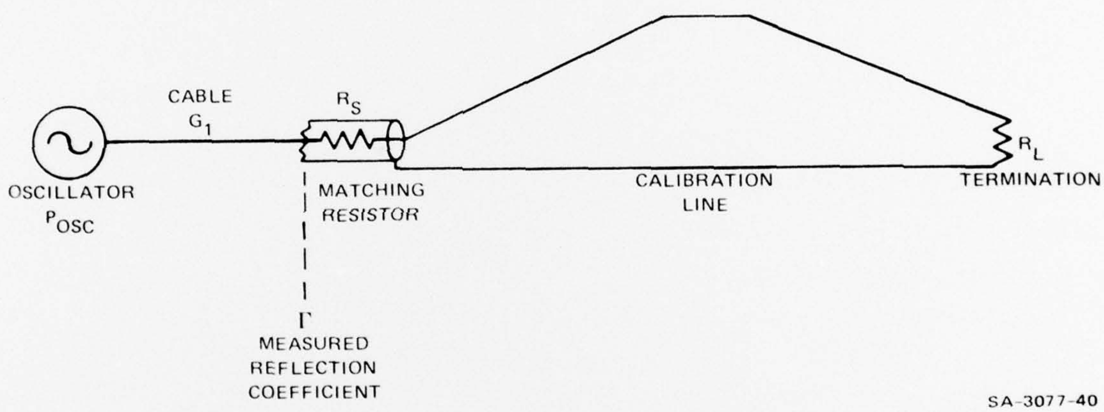

FIGURE A-6 SCHEMATIC OF CALIBRATION LINE INPUT CIRCUIT

The schematic of the oscillator connected to the calibration line is illustrated in Figure A-6. The power, P_L, in the calibration line is given by

$$P_L = P_{OSC} G_1 (1 - |\Gamma|^2) R_L / (R_L + R_S)$$

where G_1 is the power gain in the cable between the oscillator and the input absorbing section to the tapered line, Γ is the reflection coefficient measured at the input to the calibration line including R_S. The gain in the cable is less than one and represents losses. The voltage

developed across the plates of the device is the square root of the product of the power in the field, P_L, and the characteristic resistance, R_L, of the device. Since the electric field, E_L, is the voltage across the plates divided by the height, h, the magnitude of the electric field may be expressed by the height of the line and the equipment parameters as

$$E_L = \frac{R_L}{h} \quad \frac{P_{OSC}G_1\left[1 - |\Gamma|^2\right]}{R_D + R_S} \quad .$$

The output voltage V_O of the probe into a 50-ohm load is the product of the effective height, h_E, of the sensor and the electric field E_L. The probe's output is propagated through a cable of power gain, G_2, to a spectrum analyzer with input resistance that matches the cable's characteristic resistance of $R_2 = 50$ ohms. The input power, P_A, to the spectrum analyzer that is displayed on the cathode ray tube is equal to $V_O^2\ G_2/R_2$ or $(E_L h_E)^2 G_2/R_2$. The effective height, h_E, of the probe is expressed in terms of equipment parameters, and measured results by eliminating E_L to give

$$h_E = \frac{h}{R_L} \quad \left[R_2(R_L + R_S)/G_1G_2(1 - |\Gamma|^2)\right] \ (P_A/P_{OSC}) \quad .$$

The calibration measurements are performed with a frequency-swept CW signal over the desired frequency range. The output of the swept frequency CW oscillator is maintained at a constant output level P_{OSC}. The cable gain, G_1G_2, and the reflected power, $|\Gamma|^2$, are measured. The output power from the sensor is measured as input power, P_A, to the spectrum analyzer over the frequency range from 10 MHz to 500 MHz.

Data for calibrating the probes were extracted for frequencies of 100, 200, 300, 400, and 500 MHz with the sensors located in the line at a distance of 70, 90, 100, and 126 cm from the input to the tapered section. Since the parallel plate section is so short, the probes are

located in the tapered sections with height, h. The output power of the oscillator, P, was maintained at +10 dBm. The extracted data and resulting effective heights are listed in Table A-1. The reflection coefficient, Γ, is small and varies because of the presence of the probe in the line but the transmitted power that is proportional to $(1-|\Gamma|^2)$ is practically constant. The effective heights determined for different frequencies and different distances, d, vary because of the standing wave pattern in the line. The averaged values for the effective heights rounded off to two significant figures are 1.1×10^{-3} V/V/m and 1.5 V/V/m for the H and E-field sensor, respectively, and are estimated to be correct within 10 percent.

The magnetic field is obtained from the H-field sensor's output voltage, V_o as measured into 50 ohms by

$$H = V_o/377h_E \quad .$$

Table A-1

CALIBRATION DATA AND EFFECTIVE HEIGHTS

S MHz	G_1G_2 dB	d cm	h cm	$\|\Gamma\|^2$ dB	H-Field Sensor P_A dBm	H-Field Sensor h_E V/V/m	E-Field Sensor P_A dBm	E-Field Sensor h_E V/V/m
100	-0.6	70	14.5	-13.0	-33.0	1.08×10^{-3}	-29.3	1.07×10^{-3}
		90	18.5	-12.5	-35.2	1.07×10^{-3}	-31.7	1.61×10^{-3}
		100	21.0	-12.3	-36.2	1.09×10^{-3}	-32.6	1.65×10^{-3}
		126	25.0	-12.3	-36.6	1.24×10^{-3}	-34.6	1.56×10^{-3}
200	-0.8	70	14.5	-11.0	-33.2	1.10×10^{-3}	-30.0	1.59×10^{-3}
		90	18.5	-14.5	-36.6	0.92×10^{-3}	-32.0	1.57×10^{-3}
		100	21.0	-14.5	-37.9	0.90×10^{-3}	-33.4	1.52×10^{-3}
		126	25.0	-12.5	-38.0	1.08×10^{-3}	-37.2	1.18×10^{-3}
300	-1.0	70	14.5	-13.0	-32.6	1.18×10^{-3}	-30.7	1.47×10^{-3}
		90	18.5	-9.0	-34.9	1.11×10^{-3}	-31.8	1.73×10^{-3}
		100	21.0	-10.5	-38.0	0.92×10^{-3}	-31.6	1.97×10^{-3}
		126	25.0	-11.0	-39.6	0.89×10^{-3}	-37.2	1.22×10^{-3}
400	-1.1	70	14.5	-10.0	-33.2	1.15×10^{-3}	-30.0	1.66×10^{-3}
		90	18.5	-16.0	-35.5	1.08×10^{-3}	-33.6	1.35×10^{-3}
		100	21.0	-12.0	-36.5	1.12×10^{-3}	-35.6	1.24×10^{-3}
		126	25.0	-15.5	-40.4	0.81×10^{-3}	-35.1	1.53×10^{-3}
500	-1.5	70	14.5	-17.0	-32.0	1.32×10^{-3}	-31.2	1.45×10^{-3}
		90	18.5	-14.0	-35.9	1.09×10^{-3}	-34.0	1.36×10^{-3}
		100	21.0	-17.0	-35.9	1.16×10^{-3}	-37.2	1.05×10^{-3}
		126	25.0	-17.5	-39.0	1.02×10^{-3}	-36.2	1.41×10^{-3}
Averaged effective heights						1.07×10^{-3}		1.49×10^{-3}

DISTRIBUTION LIST

DEPARTMENT OF DEFENSE

Defense Documentation Center
Cameron Station
12 cy ATTN: TC

Director
Defense Intelligence Agency
ATTN: DTICI, Robert I. Rubenstein

Director
Defense Nuclear Agency
3 cy ATTN: TITL, Tech. Library
ATTN: STVL
ATTN: RAEV
ATTN: TISI, Archives
ATTN: DDST

Dir. of Defense Research & Engineering
Department of Defense
ATTN: S&SS (OS)

Commander
Field Command
Defense Nuclear Agency
ATTN: FCPR

Director
Interservice Nuclear Weapons School
ATTN: Doc. Con. for LTC Byfield D. Gordon

Director
Joint Strat. Target Planning Staff, JCS
ATTN: JSAS

Chief
Livermore Division, Field Command, DNA
Lawrence Livermore Laboratory
ATTN: FCPRL

DEPARTMENT OF THE ARMY

Commander
BMD System Command
ATTN: SSC-TEN, L. L. Dickerson

Chief C-E Services Division
US Army Communications Command
ATTN: CEEO-7, Wesley T. Heath, Jr.

Dep. Chief of Staff for Research Dev. & Acq.
Department of the Army
ATTN: DAMA-CSM-N, LTC G. Ogden

Commander
Harry Diamond Laboratories
ATTN: DRXDO-TI, Tech. Lib.
ATTN: DRXDO-NP, Francis N. Wimenitz
ATTN: DRXDO-RBH, Paul A. Caldwell
ATTN: DRXDO-RCC, John A. Rosado
ATTN: DRXDO-RBH, Stewart S. Graybill
ATTN: DRXDO-EM, Robert E. McCoskey
ATTN: DRXDO-RC, Robert B. Oswald, Jr.
ATTN: DRXDO-TR, Edward E. Conrad

DEPARTMENT OF THE ARMY (Continued)

Commander
Picatinny Arsenal
ATTN: SMUPA-ND-W
ATTN: SARPA-TS-I-E, Abraham Grinoch
ATTN: SARPA-FR-E, Louis Avrami
ATTN: SMUPA-ND-N-E
ATTN: SARPA-ND-C-E, Amina Nordio

Commander
Redstone Scientific Information Center
US Army Missile Command
3 cy ATTN: Chief, Documents

Director
TRASANA
ATTN: STEWS-TE-NT, Marvin P. Squires
ATTN: ATAA-EAC, Francis N. Winans

Director
US Army Ballistic Research Labs.
ATTN: DRXBR-AM, W. R. Vanantwerp
ATTN: DRXBR-VL, John W. Kinch
ATTN: DRXBR-AM, Donald Eccleshall

Commander
US Army Electronics Command
ATTN: DRSEL-GG-TD, W. R. Werk
ATTN: DRSEL-PL-ENV, Hans A. Bomke
ATTN: DRSEL-CT-HDK, Abraham E. Cohen

Commander
US Army Foreign Science & Tech. Center
ATTN: P. A. Crowley

Commander
US Army Materiel Dev. & Readiness Command
ATTN: DRCDE-D, Lawrence Flynn

Commander
US Army Missile Command
ATTN: DRCPM-PE-EA, Wallace O. Wagner

Commander
US Army Nuclear Agency
ATTN: ATCN-W, LTC Leonard A. Sluga

Commander
US Army Test & Evaluation Command
ATTN: DRSTE-EL, Richard I. Kolchin

DEPARTMENT OF THE NAVY

Chief of Naval Operations
Navy Department
ATTN: Robert A. Blaise

Commander
Naval Electronic Systems Command
Naval Electronic Systems Command Hqs.
ATTN: Code 5032, Charles W. Neill

Commanding Officer
Naval Intelligence Support Center
ATTN: NISC-45

DEPARTMENT OF THE NAVY (Continued)

Director
Naval Research Laboratory
ATTN: Gerald Cooperstein, Code 7770
ATTN: Jack D. Brown, Code 7701
ATTN: J. Davis, Code 7750
ATTN: Doris R. Folen, Code 2627

Commander
Naval Surface Weapons Center
ATTN: Code WR43
ATTN: Code WA501, Navy Nuc. Prgms. Off.

Commander
Naval Weapons Center
ATTN: Code 533, Tech. Lib.

Commanding Officer
Naval Weapons Support Center
ATTN: Code 7024, James Ramsey

DEPARTMENT OF THE AIR FORCE

AF Weapons Laboratory, AFSC
ATTN: DYS, W. Baker
ATTN: SUL
ATTN: ELC, Charles A. Aeby
ATTN: CA, Arthur H. Guenther
ATTN: DYS, Daniel N. Payton
ATTN: ELP, Tree Section
ATTN: NT, John Darrah
ATTN: NT, Carl E. Baum
ATTN: SAT

Headquarters
Electronic Systems Division/DC
ATTN: DCD/SATIN IV

Hq. USAF/RD
ATTN: RDQSM

SAMSO/DY
ATTN: DYS, Major Larry A. Darda

SAMSO/IN
ATTN: IND, Major Darryl S. Muskin

SAMSO/MN
ATTN: MNNH, Captain William M. Carra

SAMSO/SK
ATTN: SKF, Peter H. Stadler

SAMSO/SZ
ATTN: SZJ, Captain John H. Salch

Commander in Chief
Strategic Air Command
ATTN: NRI-STINFO, Library

ENERGY RESEARCH & DEVELOPMENT ADMINISTRATION

University of California
Lawrence Livermore Laboratory
ATTN: Hans Kruger, L-96
ATTN: Tech. Info. Dept. L-3
ATTN: Donald W. Vollmer, L-154
ATTN: John Nuckolls, A Div., L-545
ATTN: Leland C. Loquist, L-154
ATTN: Donald J. Meeker, L-545
ATTN: Louis F. Wouters, L-48

ENERGY RESEARCH & DEVELOPMENT ADMINISTRATION (Continued)

Los Alamos Scientific Laboratory
ATTN: Doc. Con. for J. Arthur Freed
ATTN: Doc. Con. for Donald R. Westervelt

Sandia Laboratories
Livermore Laboratory
ATTN: Doc. Con. for Kenneth A. Mitchell, 8157

Sandia Laboratories
ATTN: Doc. Con. for Org. 2110, J. A. Hood
ATTN: Div. 5231, James H. Renken
ATTN: Doc. Con. for 5245, T. H. Martin
ATTN: Doc. Con. for Org. 9353, R. L. Parker
ATTN: Doc. Con. for 5240, Gerald Yonas
ATTN: Doc. Con. for 5220, Jack V. Walker
ATTN: Doc. Con. for 1114, Gerald W. Barr
ATTN: Doc. Con. for 3141, Sandia Rpt. Coll.

OTHER GOVERNMENT AGENCIES

Department of Commerce
National Bureau of Standards
ATTN: Sec. Officer for Appl. Rad. Div., Robert C. Placious

DEPARTMENT OF DEFENSE CONTRACTORS

Aerojet Electro-Systems Company Div.
Div. of Aerojet-General Corporation
ATTN: Thomas D. Hanscome

Aerospace Corporation
ATTN: S. P. Bower
ATTN: Richard Crolius, A2-Rm. 1027
ATTN: R. Mortensen
ATTN: Library
ATTN: V. Josephson
ATTN: J. Benveniste

Analog. Technology Corporation
ATTN: John Joseph Baum

Avco Research & Systems Group
ATTN: Research Lib., A830, Rm. 7201

Battelle Memorial Institute
ATTN: David A. Dingee

The BDM Corporation
ATTN: T. H. Neighbors

The Bendix Corporation
Communication Division
ATTN: Document Control

The Boeing Company
ATTN: Kenneth D. Friddell, MS 2R-00
ATTN: Aerospace Library
ATTN: David L. Dye, MS 87-75
ATTN: Howard W. Wicklein, MS 17-11

Charles Stark Draper Laboratory, Inc.
ATTN: Kenneth Fertig

Communications Satellite Corporation
ATTN: Sec. Off. for Andrew Meulenberg, Jr.

Computer Sciences Corporation
ATTN: Barbara F. Adams

Cutler-Hammer, Inc.
AIL Division
ATTN: Central Tech. Files, Anne Anthony

Dikewood Industries, Inc.
ATTN: L. Wayne Davis

EG & G, Inc.
Albuquerque Division
ATTN: Hilda H. Hoffman

Ford Aerospace & Communications Corp.
ATTN: Donald R. McMorrow, MS G30
ATTN: Library

Ford Aerospace & Communications Operations
ATTN: Tech. Info. Section
ATTN: Ken C. Attinger

The Franklin Institute
ATTN: Ramie H. Thompson

General Electric Company
Space Division
Valley Forge Space Center
ATTN: John L. Andrews
ATTN: Joseph C. Peden, VFSC, Rm. 4230M

General Electric Company
TEMPO-Center for Advanced Studies
ATTN: DASIAC

General Electric Company
Aerospace Electronics Systems
ATTN: W. J. Patterson, Drop 233

General Research Corporation
Washington Operations
ATTN: Allan C. Eckert

Georgia Institute of Technology
Georgia Tech. Research Institute
ATTN: R. Curry

GTE Sylvania, Inc.
Electronics Systems GRP-Eastern Div.
ATTN: James A. Waldon

GTE Sylvania, Inc.
ATTN: Herbert A. Ullman
ATTN: David P. Flood

Harris Corporation
Harris Semiconductor Division
ATTN: T. L. Clark, MS 4040

Hercules, Incorporated
Bacchus Plant
ATTN: 100K-26-W. R. Woodruff

Honeywell Incorporated
Avionics Division
ATTN: Ronald R. Johnson, A1622

DEPARTMENT OF DEFENSE CONTRACTORS (Continued)

Honeywell Incorporated
Avionics Division
ATTN: MS 725-J, Stacey H. Graff

Hughes Aircraft Company
Centinela & Teale
ATTN: Kenneth R. Walker, MS D157
ATTN: Billy W. Campbell, MS 6-E-110

Hughes Aircraft Company, El Segundo Site
ATTN: William W. Scott, MS A1080

Institute for Defense Analyses
ATTN: IDA Librarian, Ruth S. Smith

ION Physics Corporation
ATTN: Robert D. Evans
ATTN: H. Milde

IRT Corporation
ATTN: R. L. Mertz

Jaycor
ATTN: Eric P. Wenaas

Kaman Sciences Corporation
ATTN: Albert P. Bridges
ATTN: Walter E. Ware
ATTN: John R. Hoffman
ATTN: Donald H. Bryce

Litton Systems, Inc.
Guidance & Control Systems Division
ATTN: Val J. Ashby, MS 67

LTV Aerospace Corporation
Michigan Division
ATTN: Tech. Lib.

M.I.T. Lincoln Laboratory
ATTN: Leona Loughlin, Librarian A-082

Martin Marietta Aerospace
Orlando Division
ATTN: Jack M. Ashford, MP-537
ATTN: Mona C. Griffith, Lib. MP-30

Maxwell Laboratories, Inc.
ATTN: Alan C. Kolb
ATTN: Peter Korn
ATTN: Victor Fargo

McDonnell Douglas Corporation
ATTN: W. J. Ozeroff, A3-253-11
ATTN: Stanley Schneider

Mission Research Corporation
ATTN: Conrad L. Longmire
ATTN: William C. Hart

Mission Research Corporation-San Diego
ATTN: V. A. J. Van Lint

Motorola, Inc.
Government Electronics Division
ATTN: Tech. Info. Center, A. J. Kordalewski

DEPARTMENT OF DEFENSE CONTRACTORS (Continued)

National Academy of Sciences
ATTN: National Materials Advisory Board for R. S. Shane, Nat. Materials Advsy.

Northrop Corporation
Electronic Division
ATTN: Boyce T. Ahlport

Northrop Coporation
Northrop Research & Technology Center
ATTN: Orlie L. Curtis, Jr.
ATTN: Library

Northrop Coporation
Electronic Division
ATTN: Vincent R. DeMartino

Physics International Company
ATTN: Doc. Con. for Ian D. Smith
ATTN: Doc. Con. for Philip W. Spence
ATTN: Doc. Con. for Bernard H. Bernstein
ATTN: Doc. Con. for John H. Huntington
ATTN: Doc. Con. for Sidney D. Putnam
ATTN: Doc. Con. for Charles H. Stallings

University of Pittsburgh of the Comwlth. Sys. of Higher Educ.
Cathedral of Learning
ATTN: Manfred A. Biondi

Pulsar Associates, Inc.
ATTN: Carleton H. Jones, Jr.

R & D Associates
ATTN: William R. Graham, Jr.
ATTN: Leonard Schlessinger

Raytheon Company
ATTN: Gajanan H. Joshi, Radar Sys. Lab.

Raytheon Company
ATTN: Harold L. Flescher

RCA Corporation
Government Systems Division
Missile & Surface Radar
ATTN: Andrew L. Warren

RCA Corporation
Camden Complex
ATTN: E. Van Keuren, 13-5-2

DEPARTMENT OF DEFENSE CONTRACTORS (Continued)

Rockwell International Corporation
ATTN: James E. Bell, HA10
ATTN: L. H. Pinson, FB41

Science Applications, Inc.
ATTN: J. Robert Beyster

Science Applications, Inc.
Huntsville Division
ATTN: Noel R. Byrn

Simulation Physics, Inc.
ATTN: Roger G. Little

Sperry Rand Corporation
Sperry Division
ATTN: Paul Marraffino

Stanford Research Institute
ATTN: Philip J. Dolan
ATTN: Setsuo Dairiki
ATTN: William E. Scharfman

Systems, Science & Software
ATTN: David A. Meskan

Systems, Science & Software, Inc.
ATTN: Morris F. Scharff
ATTN: Andrew R. Wilson

Systron-Donner Corporation
ATTN: Harold D. Morris

Texas Instruments, Inc.
ATTN: Donald J. Manus, MS 72

Texas Tech. University
ATTN: Travis L. Simpson

TRW Defense & Space Sys. Group
ATTN: O. E. Adams, R1-1144
ATTN: Tech. Info. Center/S-1930
ATTN: R. K. Plebuch, R1-2078
ATTN: Robert M. Webb, R1-2410

TRW Defense & Space Sys. Group
San Bernardino Operations
ATTN: Earl W. Allen, 520/141
ATTN: F. B. Fay

Varian Associates, Inc.
ATTN: A-109, Howard R. Jory

Vector Research Associates
ATTN: W. A. Radasky

Westinghouse Electric Corporation
Defense & Electronic Systems Center
ATTN: Henry P. Kalapaca, MS 3525